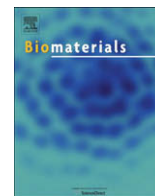




Contents lists available at ScienceDirect

Biomaterials

journal homepage: www.elsevier.com/locate/biomaterials

Self-assembled prodrugs: An enzymatically triggered drug-delivery platform

Praveen K. Vemula^{a,1}, Gregory A. Cruikshank^{b,1}, Jeffrey M. Karp^{a,*}, George John^{b,*}^aHarvard-MIT Division of Health Science and Technology, Department of Medicine, Brigham and Women's Hospital, Harvard Medical School, 65 Landsdowne Street, PRB 313 Cambridge, MA 02139, USA^bDepartment of Chemistry, The City College of New York, Convent Avenue at 138th Street, New York, NY 10031, USA

ARTICLE INFO

Article history:

Received 23 July 2008

Accepted 11 September 2008

Available online xxx

Keywords:

Prodrugs

Hydrogels

Enzyme catalysis

Self-assembly

Drug-delivery

Mesenchymal stem cells

ABSTRACT

Enzyme catalysis as a tool to disassemble supramolecular hydrogels to control the release of encapsulated drugs provides an opportunity to design a wide range of enzyme-specific low-molecular-weight hydrogelators. In this proof-of-concept work, we report the synthesis of low-molecular-weight amphiphilic prodrugs as hydrogelators from a well-known drug **acetaminophen** (which belongs to a class of drugs called analgesics (pain relievers) and antipyretics (fever reducers)). We have shown the ability of prodrugs to self-assemble to form hydrogels that could subsequently encapsulate a second drug such as curcumin, which is a known chemopreventive and anti-inflammatory hydrophobic drug. Upon enzyme-triggered degradation, the hydrogel released single or multiple drugs at physiologically simulated conditions *in vitro*. Given that the degradation products consist of the drug and a fatty acid, this approach has an advantage over polymer-based prodrugs that generate polymer fragments with heterogeneous chain lengths upon degradation that may present complex toxicity profiles. Additionally, drug-release occurred without burst release. Spectrophotometric experiments supported the drug-release, and the rate was controlled by modulation of temperature and enzyme concentration. Mesenchymal stem cells treated with prodrugs retained their stem cell properties including the capacity of multi-lineage differentiation, and maintained their adhesive and proliferation capacities with high viability. The present biomaterials could have broad applications as drug-delivery vehicles and cell invasive matrices.

Published by Elsevier Ltd.

1. Introduction

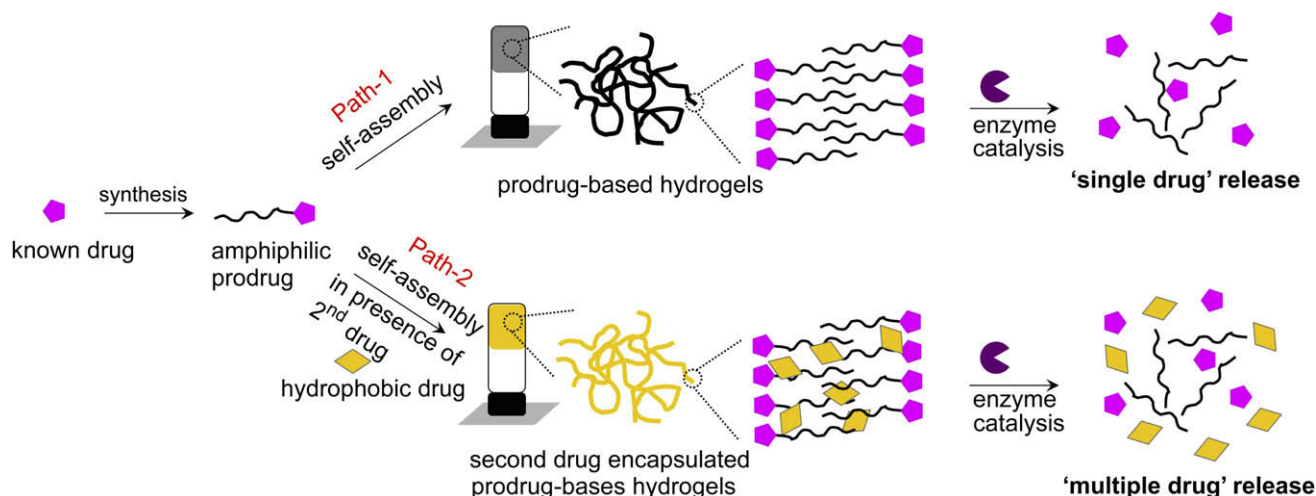
One of the fundamental problems in drug-delivery is striking a balance between toxicity and therapeutic effect. Hydrogels have been widely applied as intelligent carriers in controlled drug-delivery systems [1–6]. However, the major contribution is from polymeric hydrogels as opposed to hydrogels formed through self-assembly of low-molecular-weight gelators (LMWGs). This could be due to the relatively complex synthesis of LMWGs and concerns about possible toxicity of *in situ* generated fragments from the degradation of LMWGs. Also, self-assembled hydrogel-based drug-delivery has been hindered by the unknown fate of the host gelator after the gel degradation. Thus, we propose a conceptually novel approach to address these limitations. The existing ambiguity can be substantially decreased by designing prodrug-based LMWGs from existing drugs whose metabolic pathways are well documented. Such prodrugs should encompass key functional groups

which can promote self-assembly in aqueous solutions, and have the ability to encapsulate hydrophobic drugs within the hydrophobic pockets of hydrogel. As a result, one would develop delivery vehicles for single and multiple drugs. Upon degradation, drug encapsulated prodrug-based hydrogels could release drug-1 (which generates from cleavage of prodrug) and drug-2 (the encapsulated hydrophobic drug(s)). See **Scheme 1** for the pictorial representation of single and multiple drug-delivery from a prodrug-based hydrogel. Previously, small molecule drugs were judiciously combined with polymers [7,8]. However, polymer degradation can lead to polymer fragments with heterogeneous chain lengths that may generate potential toxicity or unwanted side effects. Our present approach (degradable prodrug-based self-assembled hydrogels) overcomes this hurdle as it degrades into pure drug with a single non-cytotoxic fatty acid upon enzyme-mediated gel degradation. In addition, this approach provides an opportunity to avoid the undesired burst release that is often the hallmark of polymer-based drug-delivery devices [9].

Self-assembled hydrogels can be formulated in a variety of physical forms, such as microparticles, nanoparticles, coatings and films. As a result, hydrogels found niche applications in clinical practice and experimental medicine for a wide range of applications, including tissue engineering and regenerative medicine [10],

* Corresponding authors.

E-mail addresses: jeffkarp@mit.edu (J.M. Karp), john@sci.ccnycunyu.edu (G. John).¹ constitutes equal contribution.



Scheme 1. Schematic representation of the preparation of degradable prodrug-based hydrogelators, encapsulation of hydrophobic drug in the gel, and subsequent enzyme-triggered single (path-1) and multiple (path-2) drug-delivery.

diagnostics [11], cellular immobilization [12], separation of biomolecules or cells [13] and barrier materials to regulate biological adhesions [14]. Hydrogels are appealing for biological applications because of their high water content and biocompatibility. In the last few decades hydrogel research has gained considerable attention and significant progress has been made in designing, synthesizing and using these materials for several biomedical applications [15–17] in particular drug-delivery [4–6]. Recent developments include the design and synthesis of novel hydrogels and their use in tissue engineering, drug-delivery and bionanotechnology [4–6,10,18–21]. However, opposed to polymer-based hydrogels, limited reports are available to generate LMWGs [22–30] probably due to their complexity in synthesis.

Drug-delivery can occur from hydrogels through mechanisms such as swelling and dissolution. Biodegradability via dissolution may be designed into hydrogels through enzymatic, hydrolytic, or environmental (e.g. pH, temperature, or electric field) pathways. One of the most interesting stimuli that can be employed for drug-release is the action of enzymes, which can permit the release of encapsulated therapeutics in desired locations. For instance, drug-release in tumors as a result of the enzymatic action of tumor-associated proteases [31–33] such as plasmin, or in selected sites of the gastro intestinal tract under the influence of digestive enzymes has been reported [34,35]. Recently, we have demonstrated enzyme-mediated synthesis as a tool to synthesize the gelators from renewable resources, and enzyme-mediated gelator degradation as stimuli for degradation of the gel which triggered drug-delivery [36]. In modifying this previous approach we have overcome existing hurdles to develop biocompatible amphiphilic prodrugs as LMWGs to encapsulate hydrophobic drugs and subsequently release single and multiple drugs upon enzyme-mediated gel degradation (Scheme 1) in this investigation. To demonstrate the proof-of-concept, we choose the well-known drug Tylenol, *N*-(4-hydroxyphenyl)acetamide, which is also known as **acetaminophen (Apn)**, its drug activity is well studied [37,38]. **Apn** is a common analgesic and antipyretic drug that is used for the relief of fever, headaches, and other minor aches and pains. It is remarkably safe in recommended doses and importantly its route of metabolism in humans has extensively been investigated and found to be safe [39]. A series of amphiphiles and bolaamphiphiles (bolaamphiphiles are amphiphilic molecules that have hydrophilic polar groups at both ends of hydrophobic hydrocarbon chain) were synthesized in a single step from **Apn** as shown in Scheme 2. The designed

Apn-based prodrugs encompass required functional groups which can promote intermolecular interactions through hydrogen-bonding, pi-pi stacking and van der Waals forces.

2. Materials and methods

2.1. Materials

2.1.1. General information

Acetaminophen and curcumin were purchased from Acros Chemicals (Fisher Scientific Company, Suwanee, GA). The Novozyme 435 [lipase B from *Candida antarctica*, (CALB)] and Lipolase 100L was obtained from Novozymes through Brenntag North America. Human MSCs were obtained from the Center for Gene Therapy at Tulane University. α -MEM, Fetal Bovine Serum, L-Glutamine and Penn-Strep were purchased from Invitrogen. All other chemicals and reagents were purchased from Sigma Aldrich (St. Louis, MO) and were used without further purification unless specified.

2.2. Synthesis of hydrogelators

In a round bottom flask, α,ω -dicarboxylic acid (12 mmol) was dissolved in dry THF, to that 1.2 equivalent of DCC and catalytic amounts of DMAP were added at room temperature. After stirring for 1 h, 4-Hydroxyacetanilide (1.36 g, 10 mmol) was added in one lot and stirring continued for 24 h. After completion of the reaction, mixture was filtered through cindered flask to remove DCU, washed with THF. After removal of THF, slightly acidic water was added, and thrice extracted with chloroform; organic layer was dried over anhydrous Na_2SO_4 . After evaporating the solvent, the obtained crude products were purified by silica gel column chromatography using methanol:chloroform (1:9) as eluent, afforded pure products as white solid. Yields of the reactions were ~50%.

For detailed synthesis procedures and characterization of compounds see Supporting Information.

2.3. Preparation of gels

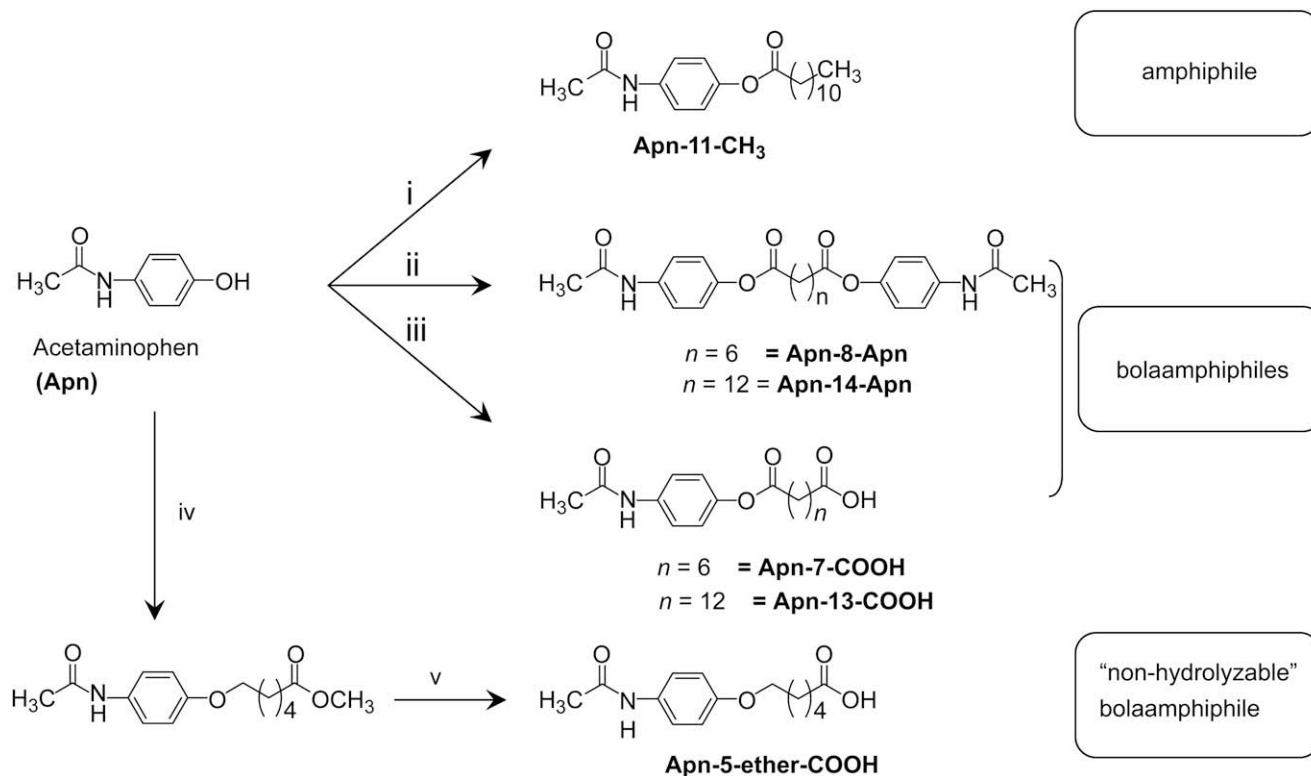
Typically, in a scintillation glass vial required solvent was taken, to that appropriate amount of gelator (0.5–5 wt/v%) was added then sealed with a screw cap. The vial was heated to ~60–80 °C until the gelator was completely dissolved. Then vial was placed at room temperature without disturbing it, typically after 15–45 min complete solution became viscous gel. Gelation was considered to have occurred when no gravitational flow was observed upon inverted tube.

2.4. Gel melting temperatures

Gel to Solution transition temperature (T_{gel}) was determined by typical 'inversion-tube-method' [23,29]. In 2 mL glass vial 1 wt/v% gelator was taken and prepared the gel as described in Section 2.3. The vial was immersed in a water bath 'up-side-down' and slowly heated, the temperature where the viscous gel melted and became solution to flow to bottom of the vial was considered as T_{gel} .

2.5. Scanning electron microscopy

To record SEM, xerogels were prepared by lyophilizing the gels (which were prepared as described in Section 2.3). Small amounts of xerogel were placed on



Scheme 2. Synthesis of amphiphiles and bolaamphiphiles from acetaminophen. Reagents and conditions: (i) dodecanoic acid, dicyclohexylcarbodiimide (DCC), dimethylamino-pyridine (DMAP), anhydrous tetrahydrofuran (THF), rt, 24 h. (ii) α,ω -dicarboxylic acid (0.5 equiv.), DCC, DMAP, dry THF, rt, 48 h. (iii) α,ω -dicarboxylic acid (1.2 equiv.), DCC, DMAP, dry THF, rt, 24 h. (iv) 6-bromomethylhexanoate, K₂CO₃, dry THF, reflux, 12 h. (v) NaOH, MeOH, rt, 12 h.

carbon-tape attached aluminum grid and coated with thin-layer of gold (50 nm) using sputtering machine. Those aluminum grids were directly imaged under SEM.

2.6. Transmission electron microscopy

TEM was recorded by using Zeiss EM 902 transmission electron microscope (80 kV). A small portion of gel was drop cast on a Cu-grid. After drying the grid at ambient temperature, the sample was directly imaged under TEM.

2.7. UV-vis spectroscopy

UV-visible spectra of the amphiphiles and curcumin were recorded using CARY100BIO spectrophotometer. In all experiments, solutions were taken in quartz cuvette of 1-cm path length.

2.8. X-ray diffraction (XRD)

XRD measurements were conducted using a Bruker AXS D-8 Discover with GADDS diffractometer using graded d -space elliptical side-by-side multilayer optics, monochromated CuK α radiation (40 kV, 40 mA), and imaging plate.

2.9. Mesenchymal stem cell culture

2.9.1. General method

Primary human mesenchymal stem cells were maintained in expansion media that consisted of 15% Fetal Bovine Serum (selected for its ability to expand MSCs), 1% (v/v) L-Glutamine, 1% (v/v) Penn-Strep, and α -MEM. All experiments were performed using MSCs at passage number 4–6.

2.9.2. Viability, adhesion and proliferation characteristics

Apn-based prodrugs are not soluble in water at room temperature, hence they were dissolved in ethanol and used in the viability, adhesion and proliferation experiments. To maintain similar experimental conditions with the Apn control, Apn was dissolved in ethanol. The viability of the cells was examined using trypan blue exclusion. Briefly, cells were plated into 12 well plates, to that 250 μ m of Apn or Apn-based prodrugs were added, and incubated for 48 h at 37 °C and 5% CO₂. The media was then aspirated and the cells were detached with 200 μ L of cell dissociated solution (similar quantities of floating cells were observed between the groups, typically 5–10 per well). 300 μ L of media was added and the total 500 μ L of the cell dispersion was collected in eppendorf tubes. From this 10 μ L of cell dispersion was

diluted 1:1 with 4% trypan blue solution and cells were counted in a hemocytometer to determine the number viable (non-blue) and nonviable (blue) cells. A control for this experiment included cells treated with only phosphate buffer saline (PBS) without an Apn-amphiphile. Cell adhesion was quantified by measuring the number of adherent cells on tissue culture surfaces in 96 well plates after incubating with amphiphiles for 12 h. For proliferation studies, 5000 cells were added to each well of a 96 well plate in 200 μ L of MSC cell expansion media, and appropriate amphiphiles were then added and incubated at 37 °C and 5% CO₂. Proliferation was quantified by manually tabulating the number of cells within the flask at multiple time points (1, 2, 3, 4, 6 and 8 days) with light microscopy at 10 \times .

2.9.3. Osteogenic differentiation

MSCs were seeded in the wells of 24 well plates, and were cultured in MSC expansion media until they reached 90% confluence (note: in control samples there is no amphiphile present, whereas in experimental samples 250 μ m of Apn-based amphiphile was present (ethanolic solution of Apn-based amphiphiles used)). Osteogenic differentiation was induced by culturing the cells for 23 days in osteogenic induction media (from Lonza – MSCs Osteogenic Single Quote kit) containing dexamethasone, β -glycerophosphate, L-ascorbic acid-2-phosphate, and α -MEM. The media in both groups were changed every 3 days (note: each time while changing the media, 250 μ m of Apn-based amphiphiles were added to maintain constant concentration). Osteogenesis was evaluated by cell membrane associated alkaline phosphatase activity. Alkaline phosphatase activity was examined after 23 days by carefully aspirating the media and washing the cells with PBS. The cells were fixed with 3.7% formaldehyde solution for 15 min at room temperature followed by rinsing with distilled water. 0.06% Red Violet LB salt solution in Tris HCl was added with distilled water containing DMF and Naphthol AS MX-PO₄. The plates were incubated for 45 min at room temperature and then the wells were rinsed 3 times with distilled water and imaged with inverted phase contrast microscope.

2.9.4. Adipogenic differentiation

MSCs were seeded in the wells of 24 well plates, and were cultured in MSC expansion media until they reached 90% confluence (note: in control samples there was no amphiphile present, whereas in experimental samples 250 μ m of Apn-based amphiphile was present (ethanolic solution of Apn-based amphiphiles used)). Adipogenic differentiation was induced by culturing the cells for 23 days in adipogenic induction media (from Lonza – MSCs Adipogenic Single Quote kit containing h-Insulin (recombinant), L-Glutamine, Dexamethasone, Indomethacin, IBMX (3-isobutyl-1-methyl-xanthine), Pen/Strep) and adipogenic maintenance media (from Lonza – MSCs Adipogenic Single Quote kit containing h-Insulin (recombinant),

L-Glutamine, Pen/Strep). The media in both groups were changed every 3 days in a periodic exposure of induction and maintenance media as suggested by the supplier (Lonza), (note: each time while changing the media, another 250 μM of **Apn**-based amphiphiles were added to maintain constant concentration). Adipogenesis was evaluated by Oil Red O staining. Following aspiration of the media, cells were washed once with PBS, and fixed in PBS with 3.7% formaldehyde for 30 min at room temperature. Following fixation cells were rinsed with distilled water for a few minutes, and incubated with isopropanol containing an Oil Red O working solution (prepared by diluting 30 mL of 0.5% isopropanol/Oil Red O solution with 20 mL of distilled water). After 45 min each culture well was rinsed twice with distilled water and 1 mL of hematoxylin was added to each well for 1 min followed by aspiration and washing with distilled water. The wells were viewed using an inverted phase contrast microscope.

3. Results and discussion

3.1. Design and synthesis of prodrug-based gelators

Design of amphiphilic gelators from known drugs is a challenging task. During this process one has to consider a few key parameters; i) the drug molecule should have a reaction site which can be easily functionalized under mild conditions; ii) the functionalized drug (prodrug) should contain a moiety which promotes self-assembly, through functionality inherent to the drug or added through the inclusion of appropriate derivatives; iii) the prodrug should be capable of (reversible) defunctionalization under 'triggered' conditions to release the parent drug. Earlier, small molecular drugs were prudently combined with polymers [7,8] or polymeric micelles [40,41]. However, to best of our knowledge there are no reports on developing single and multiple drug-delivery vehicles from self-assembled prodrugs. Hence, we choose **Apn** for generating prodrug-based hydrogelators.

Though the **Apn** acetamide group can promote hydrogen-bonding and the phenyl ring can facilitate intermolecular associations through pi-pi stacking, the molecule alone is water soluble. Thus, addition of a fatty acid through a labile ester linker (**Apn-11-CH₃**) will insert the ability to form van der Waals interactions and convert the compound into an amphiphile. However, we anticipated that **Apn-11-CH₃** may not get dispersed into water upon heating due to non-polar nature of the molecule; hence we also designed more polar bolaamphiphiles (Scheme 2). Introduction of a terminal carboxyl group (**Apn-7-COOH** and **Apn-13-COOH**) renders multiple advantages such as increasing the polarity, additional hydrogen bond forming ability through carboxylic groups and possibility to control the self-assembly through pH variation. Symmetrical bolaamphiphiles were synthesized connecting two **Apn** molecules through a dicarboxylic acid linker (**Apn-8-Apn** and **Apn-14-Apn**). In addition, to probe the mechanistic properties of enzyme-triggered gel degradation and drug-delivery we have coupled a hydrocarbon chain through a non-hydrolyzable ether linker (**Apn-5-ether-COOH**, Scheme 2), which also has a terminal carboxylic group, hence can retain its self-assembling ability. **Apn**-based amphiphiles and bolaamphiphiles were synthesized using a simple synthetic strategy in a single step as shown in Scheme 2 and in the experimental section. Thus this synthetic route may provide the opportunity to develop these gelators in industrial scale for various applications.

3.2. Gelation studies with prodrug-based gelators

Gelation abilities of **Apn**-based amphiphilic prodrugs have been investigated thoroughly in a wide range of solvents (for detailed gelation results see Table S1, supplementary data). Typically, the required amount of gelator was placed in a glass vial and with appropriate solvent, subsequent heating resulted dissolution of the gelator. The resulting solution was slowly cooled to room temperature and gelation was visually observed. Gelation was confirmed

when no gravitational flow was observed in an inverted vial. All **Apn**-based amphiphiles were excellent thermoreversible gelators. Amphiphile **Apn-11-CH₃** did not gelate in water while gelating various organic solvents. Despite prolonged heating **Apn-11-CH₃** was not soluble in water. In contrast, **Apn-7-COOH** forms excellent gels in water and other aqueous buffer solutions even in the presence of salts. In addition, **Apn-7-COOH** is soluble in basic solutions (pH greater than 8). This clearly shows that terminal carboxylic acid groups play vital role in the self-assembly process through formation of hydrogen-bonding network. However, due to the longer hydrophobic chain **Apn-13-COOH** was sparingly soluble in water and thus additional co-solvent (5–15 v/v% of alcohol such as methanol, ethanol or isopropanol) is necessary to make the hydrogel. Interestingly, symmetrical bolaamphiphile **Apn-8-Apn** formed stable hydrogel while **Apn-14-Apn** required co-solvent to form hydrogel. Thus, these results clearly show that delicate balance of solvophobic and solvophilic forces is necessary while other functional groups promote intermolecular interactions such as hydrogen-bonding, pi-pi stacking and van der Waals interactions. All gelators showed low minimum gelation concentrations (between 0.4–1.5 w/v% and millimolar concentrations, Table S1, supplementary data). Gel to solution transition temperature (T_{gel}) was determined by typical inversion-tube-method [23,29], and they exhibited values between 60 and 82 °C for 1 wt% of gels depending on the solvent used. All gels were opaque in nature and stable for several weeks. These results clearly indicate that prodrug-based hydrogels do exhibit high thermal and temporal stabilities. Detailed gelation results are given in Table S1 of supplementary data.

3.3. Hydrogel morphology

The morphologies of self-assembled hydrogels were examined under scanning and transmission electron microscopy (SEM and TEM, respectively). Investigation of the hydrogels of **Apn-7-COOH** and **Apn-8-Apn** with SEM and TEM showed that prodrug gels form branched or entangled fibrous/sheet-like gel networks with fiber thickness of 50–400 nm, and fiber lengths of several microns (Fig. 1). The high aspect ratios of the gel fibers clearly indicate that the intermolecular interactions between the gelator molecules are highly anisotropic. In addition, lower gelation concentrations and high temporal stability of the gels suggest that the intermolecular interactions are more prevalent and thus most likely the result of the synergistic effect of both pi-pi interactions and hydrogen-bonding.

3.4. Self-assembly in hydrogels

We obtained optimized geometries and calculated the lengths of gelators using ab initio calculations and by combining the data from X-ray diffraction (XRD) and Fourier transform infrared spectroscopy (FT-IR) we could propose a model for self-assembly of amphiphilic prodrugs in aqueous solution. All the ab initio Hartree-Fock calculations reported in this work were performed using the Gaussian 03 suite program [42]. The geometries of **Apn-7-COOH** and **Apn-8-Apn** have been located and optimized at the level of restricted Hartree-Fock (RHF) using the 6-31G* basis set [43]. All structures were completely optimized without any symmetry restrictions. For both molecules studied, vibrational frequency calculations were carried out to confirm that they converge to true minima by diagonalization of their Hessian (force constant) matrices at the same level to make sure that all frequencies are genuine. To check the reliability of the level of theory, we have optimized **Apn** using RHF/6-31G*, thus geometrical parameters were compared with the reported crystal structure of **Apn** [44] (see Tables S2 and S3, supplementary data). Fully optimized geometries

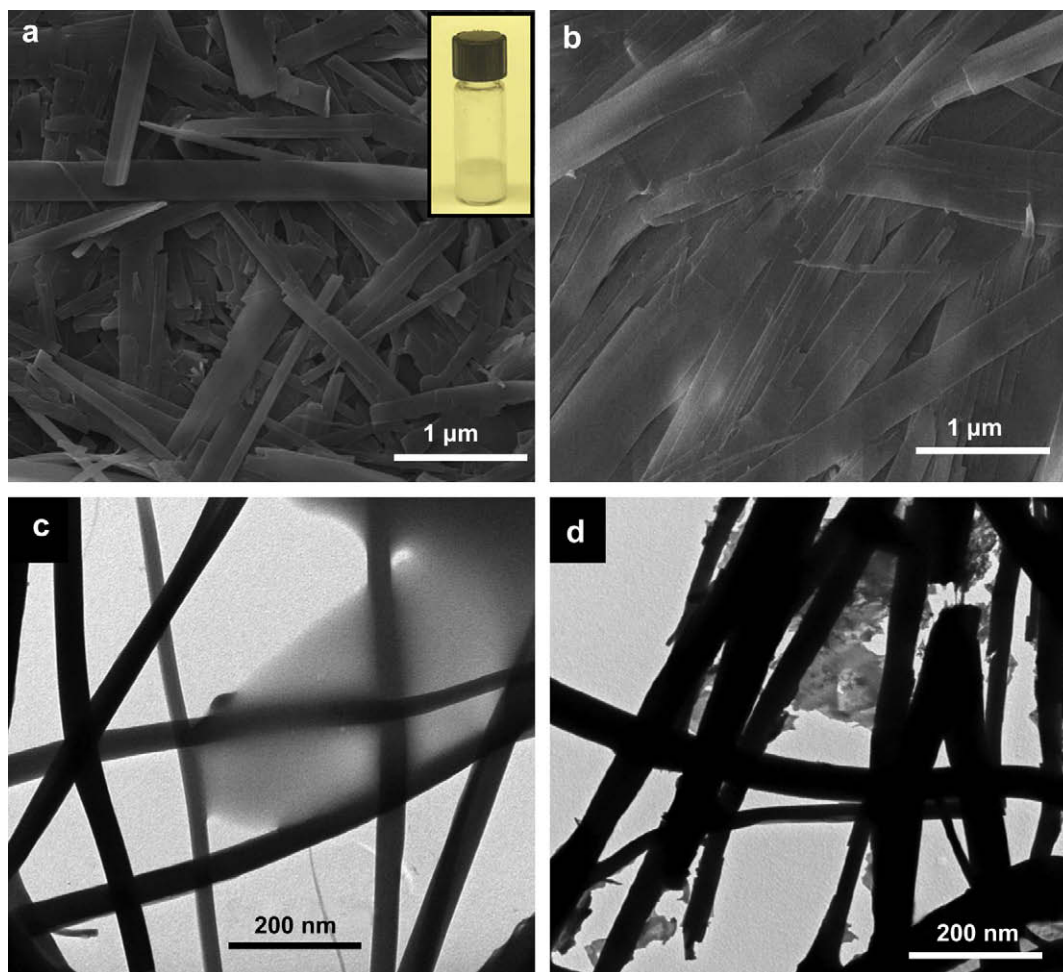


Fig. 1. Examination of hydrogel morphology with electron microscope. SEM images of hydrogels made from (a) **Apn-7-COOH**, and (b) **Apn-8-Apn**. Unstained TEM images of hydrogels made from (c) **Apn-7-COOH**, and (d) **Apn-8-Apn**. Inset shows the real image of the hydrogel.

of both amphiphilic prodrugs are shown in Fig. 2a, and calculated lengths are 1.97 and 2.67 nm for **Apn-7-COOH** and **Apn-8-Apn**, respectively.

The hydrogels obtained from prodrugs **Apn-7-COOH** and **Apn-8-Apn** displayed well-resolved X-ray diffraction (XRD) patterns that were characteristic of long-range ordering of the gelators. We calculated the long spacing (d) to postulate the possible mode of self-assembly in the gel state. Long distance spacing values suggest that possibly lamellar structures were formed by these gelators in the gels. In XRD measurements, the hydrogel of **Apn-7-COOH** showed a d of 3.53 nm, which is higher than the molecular length of **Apn-7-COOH** (1.97 nm from the optimized geometry calculations, Fig. 2a) and slightly lower than double the molecular length. Therefore, it can be predicted that **Apn-7-COOH** can self-assemble in two possible manners; one is carboxylic acids facing aqueous portion, or formation of dimer through carboxylic acids while acetaminophen facing outer side the assemblies (Fig. 2b and c, respectively). Perhaps dimeric formation of carboxylic acids could prevent the interdigitation of amphiphiles which results in the tilting of amphiphiles with respect to normal to the layer plane (Fig. 2c). Interestingly, hydrogel of **Apn-8-Apn** showed two major d values of 2.72 and 4.9 nm. In the case of $d = 2.72$ which is close to the molecular length of **Apn-8-Apn**, thus we postulate the existence of a monolayer-like structure which could be stabilized by strong intermolecular interactions such as hydrogen-bonding, pi-pi interactions as shown in Fig. 2d. Additionally, acetaminophen groups of two adjacent layers could form strong hydrogen-bonding

as shown in Fig. 2e which strongly supports the observed d value 4.9 nm. In addition, FT-IR experiments were performed to gain insight into the hydrogen-bonding environment of the amide carbonyl (C=O) group in **Apn-8-Apn** under solution and gel conditions. In the methanolic solution of **Apn-8-Apn**, an amide I band appeared at 1663 cm^{-1} whereas in gel state it shifted to 1631 cm^{-1} . Such significant shift of 32 cm^{-1} could be attributed to the strong hydrogen-bonding interactions of the carbonyl groups of acetamides in the gel state which clearly suggests that hydrogen-bonding does enhance the self-assembly of these amphiphilic prodrugs to form hydrogels. Thus, based on the information obtained from the theoretical calculations, FT-IR and XRD experimental results we propose the possible model for the self-assembly of these amphiphiles as seen in Fig. 2.

3.5. Enzyme-mediated single and multiple drug-release

Many potent therapeutic agents possess a high degree of hydrophobicity which can greatly impede their solubilization in aqueous media and thus hamper their oral or parenteral administration. In order to circumvent this limitation, it is extremely important to develop suitable biocompatible drug-delivery systems which can provide increased surface area for a therapeutic agent to dissolve in, thus, providing many hydrophobic drug molecules throughout the assembled gel. In the present work, we demonstrate the encapsulation of a hydrophobic drug in a prodrug-based hydrogel, which upon enzyme-mediated gel degradation releases

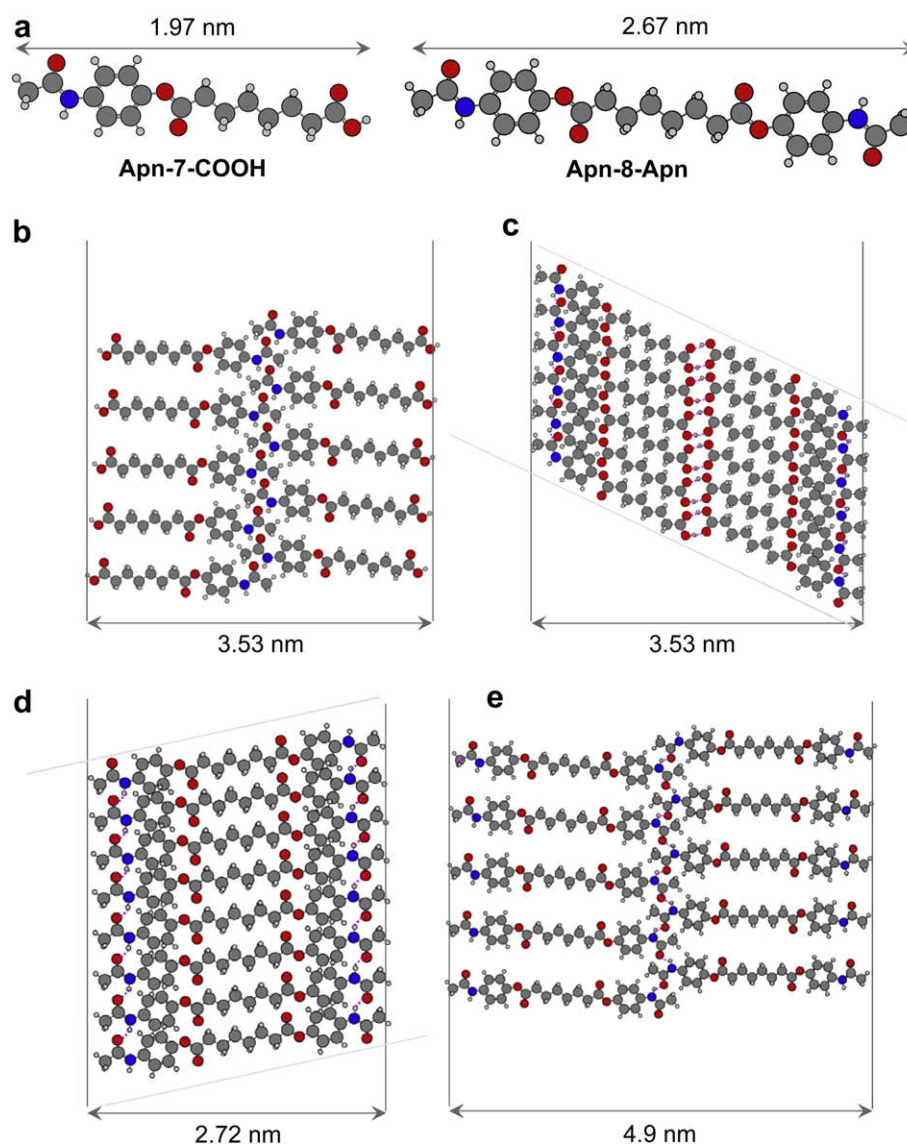


Fig. 2. Model for self-assembly of prodrug-based hydrogelators. (a) Optimized geometries of hydrogelators. Proposed mode of self-assembly into fiber based hydrogels made of (b and c) **Apn-7-COOH**, and (d and e) **Apn-8-Apn**.

single and multiple drugs at physiological conditions in a controlled manner. Earlier we have shown the enzyme-triggered controlled delivery of hydrophobic drugs [36]. Reliability of low-molecular-weight hydrogels in drug-delivery has suffered from unknown complications/toxicity of in situ formed fragments that generate from degradation of hydrogelators. Unknown metabolic pathway of those fragments is one of the major hurdles in LMWGs-based drug-delivery. Hence, developing gelators from known drugs (whose metabolic pathway has been studied extensively) would possibly overcome the present limitations in the field. As a first step toward that goal, herein we developed gelators from a commonly used drug acetaminophen (also known as Tylenol[®] whose metabolic pathway is well-known [39]).

To investigate single and multiple drug-delivery from **Apn**-based prodrug hydrogels, we choose well-known chemopreventive drug curcumin as a model hydrophobic drug for encapsulating into hydrogels. Curcumin (1,7-bis(4-hydroxy-3-methoxyphenyl)-1,6-heptadiene-3,5-dione) was originally extracted from the root of *Curcuma longa*, and it is the main constituent of the Indian spice turmeric, it gives curry sauces their characteristic yellow color. Nevertheless, the most intriguing aspect of this molecule is that it

shows a wide range of pharmaceutical activity, including potent antioxidant, anti-inflammatory, antiseptic and anti-carcinogenic properties [45–49]. It also exhibited promising therapeutic activity by inhibiting various purified human immunodeficiency virus (HIV) types [47,50,51]. Despite of the promising drug activity, curcumin has an extremely poor bioavailability due to its particularly low solubility in aqueous solutions (solubility of curcumin in water is 3×10^{-8} M) [52]. Previously, Tang et al. demonstrated increased solubility of curcumin in water by forming supramolecular host-guest complex with various cyclodextrins [52]. Hence, it would be possible to increase curcumin concentration in water by encapsulating the drug into hydrogels where abundant hydrophobic regions are available. Hydrogels of **Apn-7-COOH** or **Apn-8-Apn** were found to encapsulate high concentrations of curcumin (up to 0.5 mmol); this observed enhanced concentration of curcumin could be due to localization of hydrophobic curcumin within the hydrophobic pockets of the hydrogels three-dimensional network. To examine the effect of external drug encapsulation on the inherent morphology of the self-assembled gel, curcumin encapsulated hydrogels were examined under SEM and TEM (Fig. 3). Interestingly, encapsulation of curcumin did not affect the

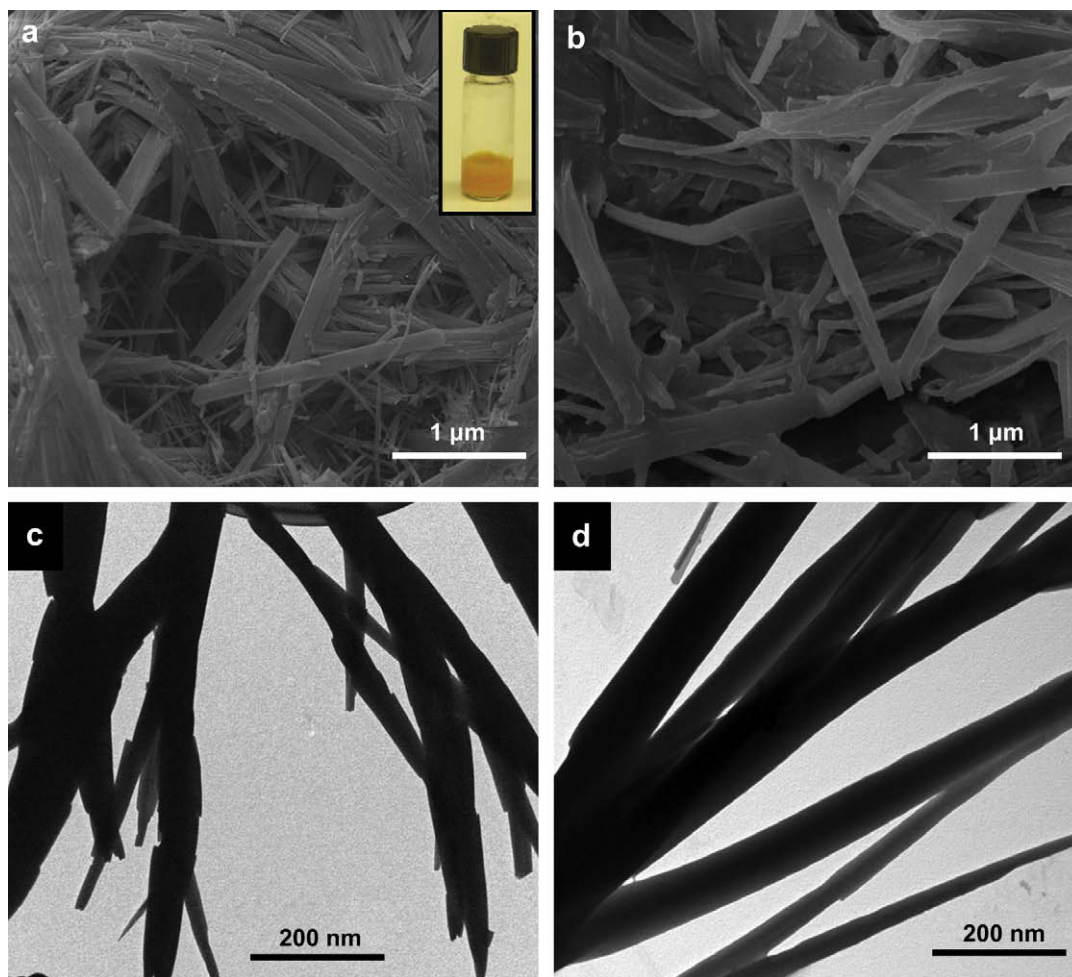


Fig. 3. Examination of drug encapsulated hydrogel morphology with electron microscope. SEM images of curcumin encapsulated hydrogels made from (a) **Apn-7-COOH**, and (b) **Apn-8-Apn**. Unstained TEM images of curcumin encapsulated hydrogels made from (c) **Apn-7-COOH**, and (d) **Apn-8-Apn**. Insets show the real image of the curcumin encapsulated hydrogel.

morphology of the hydrogels. We believe that previously suggested possible self-assembly phenomenon is identical in both types of hydrogels (with and without curcumin) as there was no significant difference in the morphology of the native hydrogels and curcumin encapsulated hydrogels (Figs. 1 and 3, respectively).

Earlier, encapsulation [53] and release [36] of curcumin were studied by the Ultra-Violet absorbance spectroscopy (λ_{\max} at 424 nm). Absorbance spectrum of modified **Apn-7-COOH** was similar to that of **Apn** (Fig. 4b). In this instance, enzyme-triggered single and multiple drug-delivery has been carried out using two sets of hydrogel samples, i.e., hydrogels of **Apn-7-COOH** and **Apn-8-Apn** with and without curcumin. In the first set, lipase (Lipolase 100L, Type EX, 100 U/mL) was added to the preformed hydrogel of **Apn-7-COOH** (2 wt%) and kept it at 37 °C which is lower than the gel melting temperature. We anticipated that lipase (esterase) would hydrolyze the ester bond of a prodrug-based gelator (**Apn-7-COOH**) to release acetaminophen and dicarboxylic acid as the hydrogel degrades (earlier, we have shown lipase-mediated ester hydrolysis and gel degradation [36]). As we expected, after 48 h the gel completely degraded and became a clear solution. However, by performing UV-absorption experiments we could not study the release of original drug acetaminophen (**Apn**) as absorbance peaks of **Apn** and lipase overlap significantly. Instead, in a traditional way, we performed thin-layer chromatography on the resulting clear solution, and found that indeed acetaminophen and α,ω -dicarboxylic acid were generated in the solution after lipase addition,

which suggests that the gel degradation is occurring through the cleavage of ester bonds within the acetaminophen-based prodrugs by lipolase enzyme.

To test this further and examine multiple (two) drug-delivery (Fig. 4), curcumin was encapsulated in the hydrogel of **Apn-7-COOH** (2 wt%) and to that, lipase was added and kept it at 37 °C. Absorbance spectra were recorded on aliquots which were collected (after the addition of enzyme to the hydrogel) at regular intervals (Fig. 4c). Plotting absorbance % of curcumin release vs time (inset of Fig. 4c) reveals absence of burst release which is otherwise a routine hurdle in hydrogel-based drug-release [9]. Interestingly, initial aliquots did not show any absorbance peak, but aliquots collected after 4 h showed absorption maxima at 425 nm, which corresponds to the absorption peak of curcumin. It is important to note that the concentration of the enzyme (100 U/mL) used in these in vitro experiments is higher than physiological concentration of esterases (for example, the physiological concentration of cholesterol esterase is 7 U/ml [54]). Hence we anticipate that under in vivo conditions the present system would show prolonged, sustained release. To determine the role of the enzyme on hydrogel degradation, similar experiments were performed by adding only buffered solution without an enzyme. As we expected curcumin encapsulated gel was still intact over a month, there was no visual change in the gel volume and added solution, and no absorbance peaks corresponding to the curcumin were observed suggesting that the enzyme is

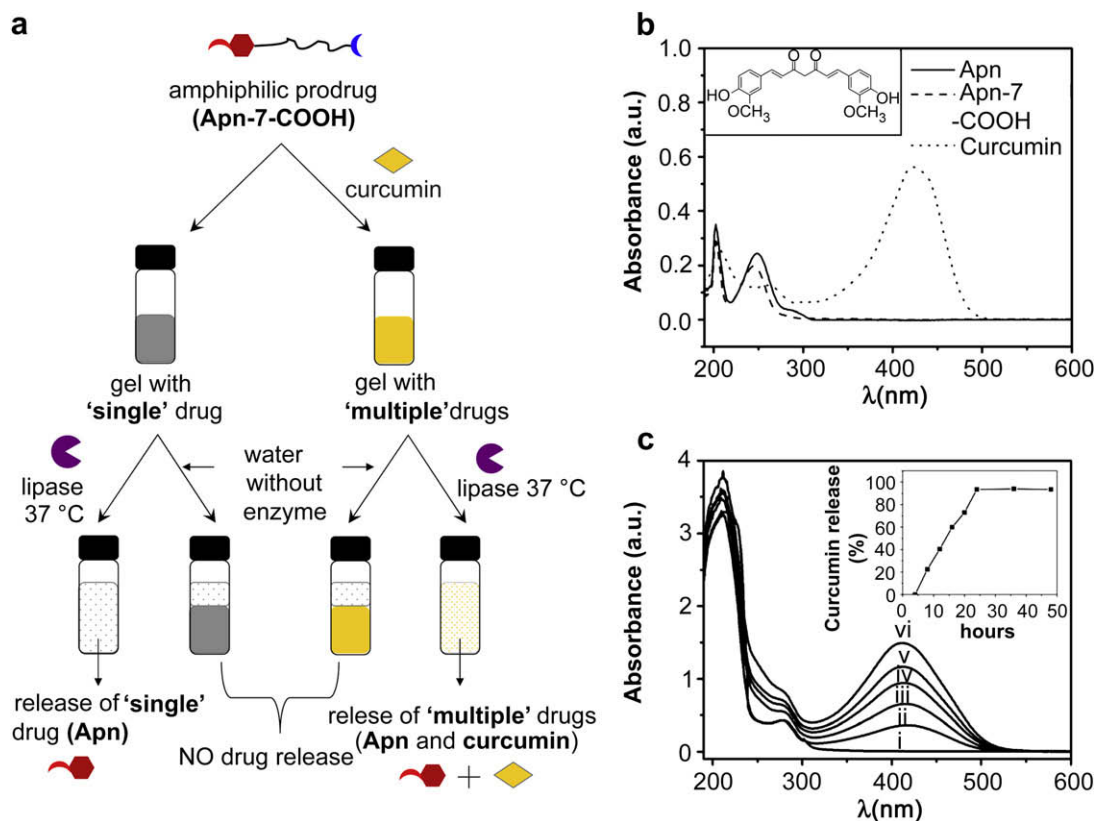


Fig. 4. Enzyme-triggered single and multiple drug-delivery. (a) Schematic representation of enzyme-mediated single and two drug-delivery from **Apn**-based prodrug hydrogels. (b) Absorbance spectra for methanolic solution of hydrogelators and curcumin. (c) Absorption spectra of curcumin released from degradation of **Apn-7-COOH** hydrogel at different time points, i) 4, ii) 8, iii) 12, iv) 16, v) 20 and vi) 24 h (after 24 h absorbance did not increase). Inset of (b) is chemical structure of curcumin, and inset of (c) is % of curcumin release vs time.

required for gel degradation. In addition, it also suggests that the curcumin release which was observed in the previous example is due to degradation of hydrogel and there was no loosely absorbed curcumin on the surface of the hydrogel diffusing into the water with time. Hence, we believe that the encapsulated curcumin intercalates within the hydrophobic pockets of self-assembled fibers. The yellow colored clear solution which was obtained after enzyme-mediated gel degradation was also tested by thin-layer chromatography, and found that **Apn** and curcumin are present; thus, it indeed confirms the synergistic release of **Apn** and curcumin which clearly indicates that with this present approach one could develop delivery vehicles to release two drugs (possibly complimentary drugs) simultaneously. Interestingly, increasing either the concentration of enzyme or incubation temperature to 45 °C doubles the drug-release rate which correlates with our previous findings [36]. Importantly, to shine the light on gel degradation mechanism we have synthesized another prodrug **Apn-5-ether-COOH** (Scheme 2), where hydrocarbon chain (which is bearing terminal carboxylic acid) was connected to the acetaminophen through an ether bond (C–O–C) to prevent the esterolytic cleavage by lipase. **Apn-5-ether-COOH** exhibited gelation behavior akin to **Apn-7-COOH**; curcumin has been encapsulated into **Apn-5-ether-COOH** hydrogel, and to that lipase was added. After incubating at 37 °C for several days, still hydrogel was in intact and prevented curcumin release into the solution (confirmed by absorption spectroscopy) which clearly suggests that indeed lipase cleaves the prodrug gelator at ester bond to release **Apn** and encapsulated curcumin. Hence, having an enzymatically cleavage labile ester group is essential to prepare the prodrug-based hydrogelators.

3.6. Cytocompatibility

Indeed, it is essential to investigate the cytocompatibility of prodrugs which are generated from small modification of known drugs. It is crucial to demonstrate that chemical modification to **Apn** did not introduce cytotoxicity into the molecule. To test the cytocompatibility of prodrug-based amphiphiles and bolaamphiphiles, and their effect on cell characteristics such as viability, proliferation, adhesion and cell phenotype, a series of experiments were performed with mesenchymal stem cells (MSCs). Given our focus to create a controlled drug-release platform that would likely be appropriate for delivery within connective tissues, we examined the impact of the amphiphiles on MSCs, which are connective tissue progenitor cells that are highly sensitive to alternations in their microenvironment. To gain more insight into the effect of modification, we used unmodified drug **Apn** as a control. Therefore, the viability of control cells and cells treated with **Apn**, **Apn-7-COOH** and **Apn-8-Apn** was examined with trypan blue assay. The presented results (Fig. 5a) suggest that there was no significant decrease in the viability of the MSCs after 48 h incubation with prodrug-based amphiphiles. Specifically, 95% of untreated cells were viable after 48 h, whereas 91%, 87% and 82% of viable cells were observed for cells incubated with 250 μM of **Apn**, **Apn-7-COOH** and **Apn-8-Apn**, respectively (Fig. 5a).

In another set of experiments, we found that viability rates were not significantly affected by a wide range of concentration of **Apn-7-COOH** (up to 500 μM , Fig. 5b). These results clearly show that **Apn**-derived prodrug amphiphiles did not induce cell toxicity. To test, how prodrug hydrogelators will affect the extracellular environment of MSCs, cell adhesion characteristics were examined

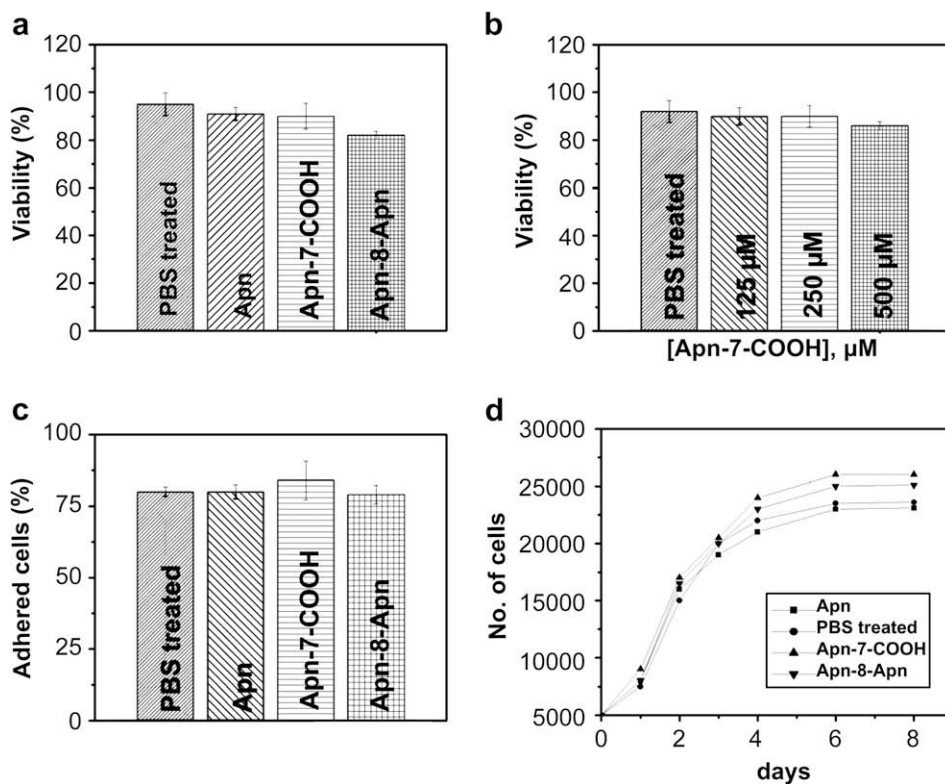


Fig. 5. Effect of prodrug hydrogels on cell characteristics. Examination of the affect of **Apn**-based prodrugs on MSCs cellular properties such as (a and b) viability, (c) adhesion, and (d) proliferation. Cell viability was examined after 48 h (a and b), adhesion was measured after 12 h (c). Concentration of **Apn** and other amphiphiles used in a, c and d are 250 μM .

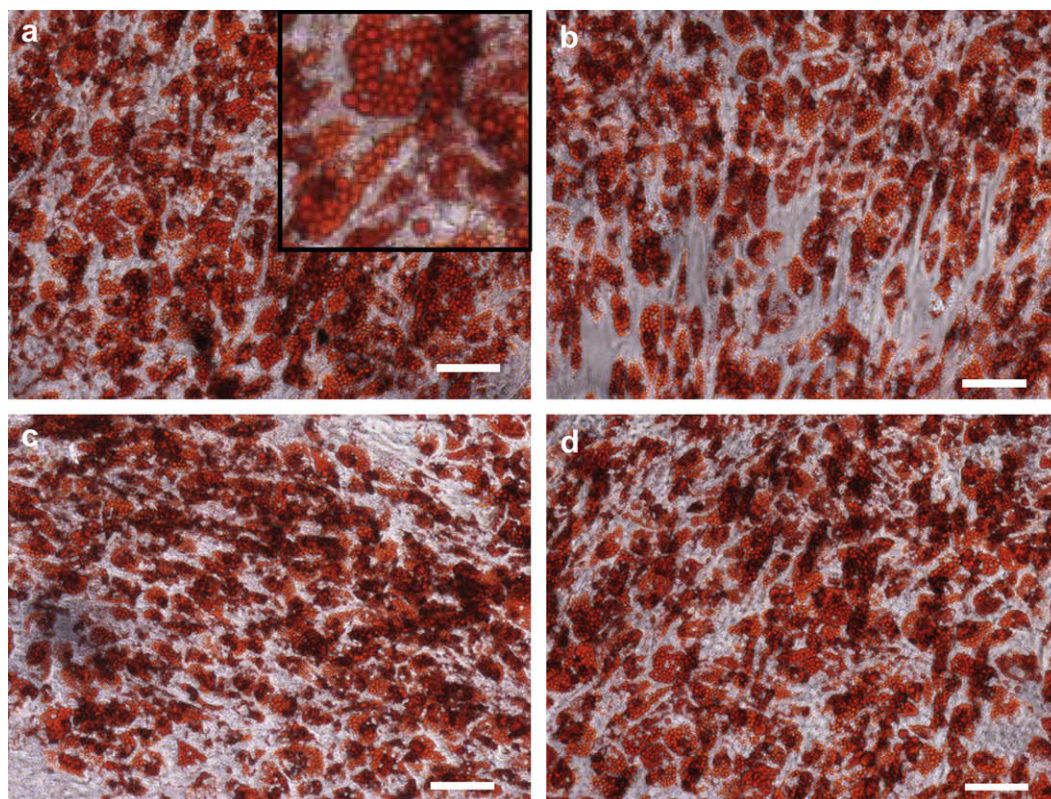


Fig. 6. Examining the cell phenotype of MSCs. After 23 days of induction adipogenesis was observed by Oil Red O (ORO) staining. Control cells treated with phosphate buffer saline (PBS) (a), and 250 μM **Apn** (b) showed positive staining. Cells treated with 250 μM of **Apn-7-COOH** (c) and **Apn-8-Apn** (d) were also equally stained for ORO. Inset of (a) shows the magnified region of fat droplets. In all images scale bar = 100 μm .

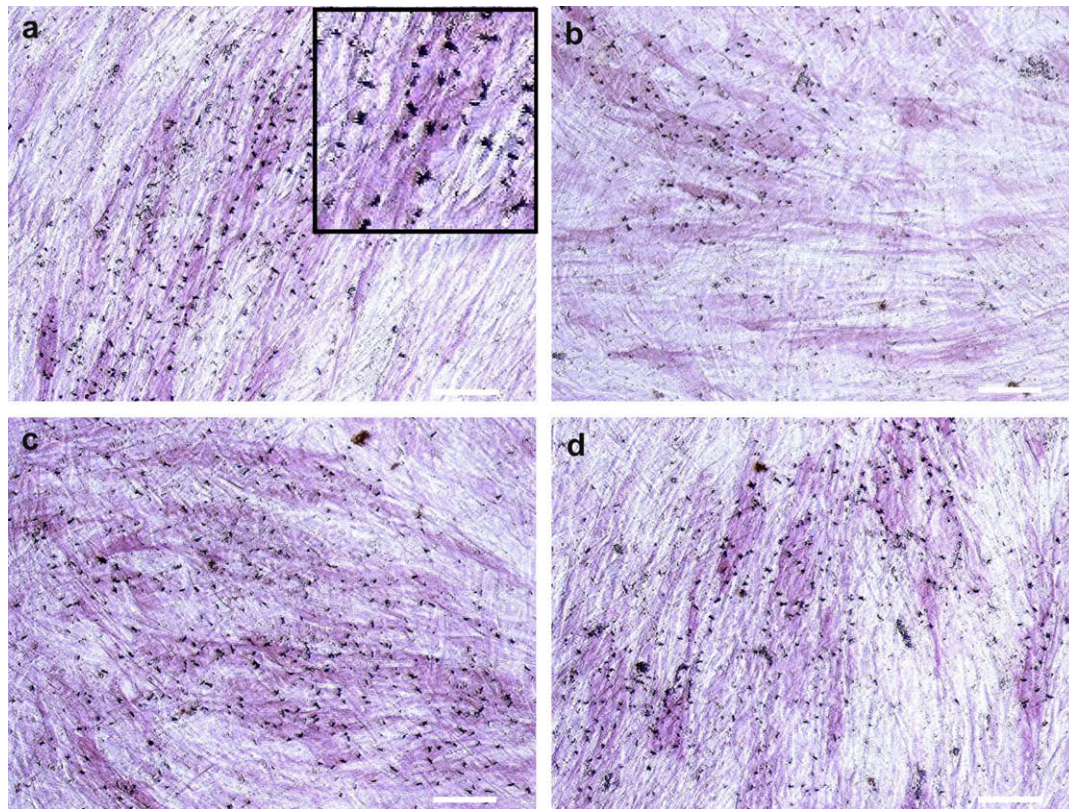


Fig. 7. Examining the cell phenotype of MSCs. After 23 days of induction osteogenesis was observed by alkaline phosphatase (ALP) staining. Control cells treated with phosphate buffer saline (PBS) (a), and 250 μM **Apn** (b) were showed positive staining. Cells treated with 250 μM of **Apn-7-COOH** (c) and **Apn-8-Apn** (d) were also equally stained for ALP. Inset of (a) shows the magnified region of differentiated cells, and black spots are mineralized foci localized to ALP stained cells. In all images scale bar = 100 μm .

(after 12 h), and found that in presence of **Apn**-based amphiphiles there was no considerable change in adhesion properties of MSCs (Fig. 5c). We also examined the proliferation rate of MSCs. In all cases (cells treated with buffer and cells treated with **Apn**, **Apn-7-COOH** and **Apn-8-Apn**) cells proliferated to attain a confluent layer, and were found to have similar proliferation rates (Fig. 5d). This indicates that, the presence of prodrug amphiphiles did not alter the proliferation of MSCs. In all experiments, ethanol was used to dissolve amphiphiles, hence the total volume of the ethanol is 1 v/v% in the experiment. To exclude the possibility that observed small changes in viability, adhesion and proliferation results were caused by ethanol, in every experiment we had control where cells were treated with 1 v/v% of ethanol. Results (not shown here) demonstrated that ethanol did not significantly affect the viability, adhesion and proliferation.

Unlike typical fibroblast cell lines used for toxicity screening, cultured mesenchymal stem cells are highly sensitive to the presence of soluble factors and can often lose their capacity for multi-lineage differentiation or differentiate into non-desired lineages depending on the culture conditions [55]. To examine the impact of the acetaminophen amphiphilic prodrugs on multi-lineage differentiation of MSCs, we treated cells with adipogenic and osteogenic induction media in presence of amphiphiles followed by respective colorimetric histological staining. Interestingly, even in the presence of **Apn**, **Apn-7-COOH** and **Apn-8-Apn**, the MSCs showed a robust capacity to differentiate into adipogenic (Fig. 6) and osteogenic (Fig. 7) lineages as shown by oil red O (ORO) staining and alkaline phosphatase (ALP) activity, respectively. No significant difference in ORO or ALP staining was observed for MSCs treated with and without **Apn**-based prodrug amphiphiles. Thus, the modified prodrugs did not impair the potential for multi-lineage differentiation. Hence, the **Apn**-based prodrugs are

cytocompatible and did not amend the inherent cellular properties of MSCs which suggest the possibility of using these amphiphiles for in vivo experiments in future research.

4. Conclusion

To summarize this work, amphiphilic low-molecular-weight prodrug hydrogelators have been synthesized from a simple modification of the known drug acetaminophen by combining a non-cytotoxic fatty acid. These prodrugs exhibited excellent self-assembling properties to generate molecular hydrogels at low concentrations. The mode of self-assembly in hydrogels was proposed based on the XRD, FT-IR data and theoretical calculations. Interestingly, we also showed the encapsulation of chemo-preventive curcumin in the hydrogels which were prepared from **Apn**-based prodrugs, and enzyme-triggered gel degradation was performed to achieve single and multiple drug-delivery in vitro at physiological conditions. In addition, we also found that all modified **Apn**-based prodrugs are excellent cytocompatible amphiphiles, and did not alter mesenchymal stem cell properties such as viability, adhesion, proliferation and ability to differentiate into multiple lineages including adipogenic and osteogenic. Based on the output of this present work, we believe that developing self-assembled hydrogelators from existing drugs which have known metabolic pathway will have broad impact in the field of 'low-molecular-weight hydrogelators-based drug-delivery'.

Acknowledgements

This work was supported (in part) by a grant from the City University of New York PSC-CUNY research award program. We thank Brenntag North America for the gift of enzyme samples.

We thank CCNY interdepartmental imaging facility for SEM and Jorge Morales for his help.

Appendix. Supplementary material

Supplementary data associated with this article can be found, in the online version, at [10.1016/j.biomaterials.2008.09.045](https://doi.org/10.1016/j.biomaterials.2008.09.045).

Appendix

Figures with essential color discrimination. Certain figures in this article, in particular Figs. 2, 4, 6 and 7, are difficult to interpret in black and white. The full color images can be found in the on-line version, at doi: [10.1016/j.biomaterials.2008.09.045](https://doi.org/10.1016/j.biomaterials.2008.09.045).

References

- [1] Peppas NA, editor. Hydrogels in medicine and pharmacy. Boca Raton, FL: CRC; 1987.
- [2] Peppas NA, Bures P, Leobandung W, Ichikawa H. Hydrogels in pharmaceutical formulations. *Eur J Pharm Biopharm* 2000;50:27–46.
- [3] Podual K, Doyle FJ, Peppas NA. Glucose-sensitivity of glucose oxidase-containing cationic polymer hydrogels having poly(ethylene glycol) grafts. *J Controlled Release* 2000;61:9–17.
- [4] Gupta P, Vermani K, Garg S. Hydrogels: from controlled release to pH-responsive drug delivery. *Drug Discov Today* 2002;7:569–79.
- [5] Miyata T, Uragami T, Nakamae K. Biomolecule-sensitive hydrogels. *Adv Drug Deliv Rev* 2002;54:79–98.
- [6] Qiu Y, Park K. Environment-sensitive hydrogels for drug delivery. *Adv Drug Deliv Rev* 2001;53:321–39.
- [7] Bryers JD, Jarvis RA, Lebo J, Prudencio A, Kyriakides TR, Uhrich K. Biodegradation of poly(anhydride-esters) into non-steroidal anti-inflammatory drugs and their effect on *Pseudomonas aeruginosa* biofilms in vitro and on the foreign-body response in vivo. *Biomaterials* 2006;27:5039–48.
- [8] Erdmann L, Macedo B, Uhrich KE. Degradable poly(anhydride ester) implants: effects of localized salicylic acid release on bone. *Biomaterials* 2000;21:2507–12.
- [9] Huang X, Brazel CS. On the importance and mechanisms of burst release in matrix-controlled drug delivery systems. *J Controlled Release* 2001;73:121–36.
- [10] Lee KY, Mooney DJ. Hydrogels for tissue engineering. *Chem Rev* 2001;101:1869–80.
- [11] van der Linden HJ, Herber S, Olthuis W, Bergveld P. Stimulus-sensitive hydrogels and their applications in chemical (micro)analysis. *Analyst* 2003;128:325–31.
- [12] Jen AC, Wake MC, Mikos AG. Review: hydrogels for cell immobilization. *Bio-technol Bioeng* 1996;50:357–64.
- [13] Wang K, Burban J, Cussler E. Hydrogels as separation agents. *Responsive gels: volume transitions II*. 1993; 67–79.
- [14] Bennett SL, Melanson DA, Torchiana DF, Wiseman DM, Sawhney AS. Next-generation hydrogel films as tissue sealants and adhesion barriers. *J Cardiovasc Surg* 2003;18:494–9.
- [15] Peppas NA, Hilt JZ, Khademhosseini A, Langer R. Hydrogels in biology and medicine: from molecular principles to bionanotechnology. *Adv Mater* 2006;18:1345–60, and references therein.
- [16] Hoare TR, Kohane DS. Hydrogels in drug delivery: progress and challenges. *Polymer* 2008;49:1993–2007.
- [17] Lu S, Anseth KS. Photopolymerization of multilaminated poly(HEMA) hydrogels for controlled release. *J Controlled Release* 1999;57:291–300.
- [18] Yang Z, Liang G, Xu B. Enzymatic hydrogelation of small molecules. *Acc Chem Res* 2008;41:315–26, and references therein.
- [19] Yang Z, Liang G, Wang L, Xu B. Using a kinase/phosphatase switch to regulate a supramolecular hydrogel and forming the supramolecular hydrogel in vivo. *J Am Chem Soc* 2006;128:3038–43.
- [20] van Bommel KJC, Stuart MCA, Feringa BL, van Esch J. Two-stage enzyme mediated drug release from LMWG hydrogels. *Org Biomol Chem* 2005;3:2917–20.
- [21] Friggeri A, Feringa BL, van Esch J. Entrapment and release of quinoline derivatives using a hydrogel of a low molecular weight gelator. *J Controlled Release* 2004;97:241–8.
- [22] Vemula PK, Aslam U, Mallia VA, John G. In situ synthesis of gold nanoparticles using molecular gels and liquid crystals from vitamin-c amphiphiles. *Chem Mater* 2007;19:138–40.
- [23] Vemula PK, John G. Smart amphiphiles: hydro/organogelators for in situ reduction of gold. *Chem Commun* 2006;2218–20.
- [24] Bhattacharya S, Maitra U, Mukhopadhyay S, Srivastava A. In: Terech P, Weiss RG, editors. *Molecular gels*. The Netherlands: Kluwer Academic Publishers; 2004.
- [25] Estroff LA, Hamilton AD. Effective gelation of water using a series of bis-urea dicarboxylic acids. *Angew Chem Int Ed* 2000;39:3447–50.
- [26] Wang G, Hamilton AD. Low molecular weight organogelators for water. *Chem Commun* 2003;310–1.
- [27] Kobayashi H, Friggeri A, Koumoto K, Amaike M, Shinkai S, Reinhoudt DN. Molecular design of “super” hydrogelators: understanding the gelation process of azobenzene-based sugar derivatives in water. *Org Lett* 2002;4:1423–6.
- [28] Sreenivasachary N, Lehn J-M. Gelation-driven component selection in the generation of constitutional dynamic hydrogels based on guanine-quartet formation. *Proc Natl Acad Sci U S A* 2005;102:5938–43.
- [29] Menger FM, Caran KL. Anatomy of a gel. Amino acid derivatives that rigidify water at submillimolar concentrations. *J Am Chem Soc* 2000;122:11679–91.
- [30] Luboradzki R, Gronwald O, Ikeda M, Shinkai S, Reinhoudt DN. An attempt to predict the gelation ability of hydrogen-bond-based gelators utilizing a glycoside library. *Tetrahedron* 2000;56:9595–9.
- [31] Curran S, Murray GI. Matrix metalloproteinases: molecular aspects of their roles in tumour invasion and metastasis. *Eur J Cancer* 2000;36:1621–30.
- [32] Trouet A, Passioskov A, van Derpoorten K, Fernandez AM, Abarca-Quinones J, Baurian R, et al. Extracellularly tumor-activated prodrugs for the selective chemotherapy of cancer: application to doxorubicin and preliminary in vitro and in vivo studies. *Cancer Res* 2001;61:2843–6.
- [33] Rooseboom M, Commandeur JNM, Vermeulen NPE. Enzyme-catalyzed activation of anticancer prodrugs. *Pharmacol Rev* 2004;56:53–102.
- [34] Chourasia MK, Jain SK. Pharmaceutical approaches to colon targeted drug delivery systems. *J Pharm Pharm Sci* 2003;6:33–66.
- [35] Sinha VR, Kumaria R. Microbially triggered drug delivery to the colon. *Eur J Pharm Sci* 2003;18:3–18.
- [36] Vemula PK, Li J, John G. Enzyme catalysis: tool to make and break amygdalin hydrogelators from renewable resources: a delivery model for hydrophobic drugs. *J Am Chem Soc* 2006;128:8932–8.
- [37] Pina LA, Sandrini M, Vitale G. The antinociceptive action of paracetamol is associated with changes in the serotonergic system in the rat brain. *Eur J Pharmacol* 1996;308:31–40.
- [38] Boutaud O, Aronoff DM, Richardson JH, Marnett LJ, Oates JA. Determinants of the cellular specificity of acetaminophen as an inhibitor of prostaglandin H₂ synthases. *Proc Natl Acad Sci U S A* 2002;99:7130–5.
- [39] Brodie BB, Axelrod J. The fate of acetanilide in man. *J Pharmacol Exp Ther* 1948;94:29–38.
- [40] Hans M, Shimoni K, Danino D, Siegel SJ, Lowman A. Synthesis and characterization of mPEG-PLA prodrug micelles. *Biomacromolecules* 2005;6:2708–17.
- [41] Kim SC, Kim DW, Shim YH, Bang JS, Oh HS, Wan-Kim S, et al. In vivo evaluation of polymeric micellar paclitaxel formulation: toxicity and efficacy. *J Controlled Release* 2001;72:191–202.
- [42] Frisch MJ, Trucks GW, Schlegel HB, Scuseria GE, Robb MA, Cheeseman JR, et al. *Gaussian 03*, revision B.03. Pittsburg, PA: Gaussian, Inc.; 2003.
- [43] Hehre WJ, Radom L, Schleyer PVR. *Ab initio molecular orbital theory*. New York: Wiley & Sons; 1986. For description of basis sets and references, see p. 63–91.
- [44] Naumov DY, Vasilchenko MA, Howard JAK. The monoclinic form of acetaminophen at 150K. *Acta Crystallogr* 1998;C54:653–5.
- [45] Jovanovic SV, Boone CW, Steenken S, Trinoga M, Kasky RB. How curcumin works preferentially with water soluble antioxidants. *J Am Chem Soc* 2001;123:3064–8.
- [46] Duvoix A, Romain B, Sylvie D, Michael S, Franck M, Estelle H, et al. Chemopreventive and therapeutic effects of curcumin. *Cancer Lett* 2005;223:181–90.
- [47] Hergenbahn M, Ubaldo S, Annette W, Axel P, Chih-Hung H, Ann-Lii C, et al. The chemopreventive compound curcumin is an efficient inhibitor of Epstein-Barr virus BZLF1 transcription in Raji DR-LUC cells. *Mol Carcinog* 2002;33:137–45.
- [48] Dahl TA, Bilski P, Reszka KJ, Chignell CF. Photocytotoxicity of curcumin. *Photochem Photobiol* 1994;59:290–4.
- [49] Shim JS, Kim JH, Cho HY, Yum YN, Kim SH, Park H-J, et al. Irreversible inhibition of CD13/aminopeptidase N by the antiangiogenic agent curcumin. *Chem Biol* 2003;10:695–704.
- [50] Mazumder A, Raghavan K, Weinstein J, Kohn KW, Pommier Y. Inhibition of human immunodeficiency virus type-1 integrase by curcumin. *Biochem Pharmacol* 1995;49:1165–70.
- [51] Sui Z, Salto R, Li J, Craik C, Ortiz de Montellano PR. Inhibition of the HIV-1 and HIV-2 proteases by curcumin and curcumin boron complexes. *Bioorg Med Chem* 1993;1:415–22.
- [52] Khodpe SM, Priyadarsini KI, Palit DK, Mukherjee T. Effect of solvent on the excited-state photophysical properties of curcumin. *Photochem Photobiol* 2000;72:625–31.
- [53] Tang B, Ma L, Wang H-Y, Zhang G-Y. Study on the supramolecular interaction of curcumin and β -cyclodextrin by spectrophotometry and its analytical application. *J Agric Food Chem* 2002;50:1355–65.
- [54] Christenson EM, Patel S, Anderson JM, Hiltner A. Enzymatic degradation of poly(ether urethane) and poly(carbonate urethane) by cholesterol esterase. *Biomaterials* 2006;27:3920–6.
- [55] Jahagirdar BN, Verfaillie CM. Multipotent adult progenitor cell and stem cell plasticity. *Stem Cell Rev* 2005;1:53–9.